Original Research Article

Effect of Boehmite Nanoparticles Surface Adsorbed with Vanadium on the Microstructure and Hardness of the Melted Zone in the Submerged Arc Welding Process

ABSTRACT

One of the most important weld quality characteristics related to the strength of the weld is the hardness of melted zone (HMZ) that is affected by different input parameters in the submerged arc welding process. In recent years, expensive nanomaterials have been effectively used in improving the quality of products in various fields. Keeping this in mind, it was therefore, decided to use a cost-effective approach to extract expensive and poisonous vanadium, from the hazardous wastewater collected from the Bistoon thermal power plant in Kermanshah province in Iran, and then introduce it into the weld pool via the cheap boehmite nanoparticles to investigate its impact on the HMZ. A five-level five-factor rotatable central composite design was then employed for collecting data in modeling of the HMZ as a function of arc voltage (V), welding current (I), stick-out (N), welding speed (S), and thickness of boehmite nanoparticles surface adsorbed with vanadium (F) coated on low-carbon steel plates (St37) prior to actual welding. The results showed that the addition of boehmite nanoparticles surface adsorbed with vanadium increased the HMZ by 13 % approximately.

Keywords: Boehmite nanoparticles; Hardness; Submerged arc welding; Vanadium.

1. INTRODUCTION

The submerged arc welding (SAW) process is generally used in the manufacturing of thick plates in pressure vessels and line pipes due to its inherent advantages such as high deposition rate, and deep penetration. Several parameters affect the properties of the weld puddle. Arc voltage,

UNDER PEER REVIEW

current and welding speed are some of these parameters that could give optimum results by controlling them [1]. Another way for obtaining better properties, especially in microstructure, is to input various elements into the puddle to improve hardness, toughness, penetration, and other properties of weld [2–4]. In this way, typical materials, micro-particles, and nanoparticles can be used [5–8]. It has been shown that in the SAW process, hardness decreases by adding TiO_2 nanoparticles to the weld pool [9]. Using nano-marbles of $CaCO_3$ in the electrode coating of the SMAW process led to an increase the hardness of weldments [7]. Despite the aforementioned investigations, there is still a lot of research to be done on the impact of nanomaterials on welding processes. Therefore in this investigation, boehmite nanoparticles surface adsorbed with vanadium (BNV) has been used for obtaining the optimum HMZ. At any temperature, vanadium with a body-centered cubic structure may be dissolved in steel. Steel also contains a small amount of carbon and nitrogen, which reacts with vanadium to generate carbide and nitride precipitates [10]. Jiang et al. [11] reported that an increase in the amount of vanadium improved the hardness and the microstructure of deposited metals changed from austenite to the mixture of austenite and martensite. Another research showed that by increasing the content of vanadium from 0 to 0.18 %, the yield strength and ultimate tensile strength progressively increased in steel bars [12].

Furthermore, the knowledge of how welding input parameters would affect HMZ is important since proper selection of these parameters affects mechanical properties and therefore, improves the quality and productivity of weldments in the welding industry. Several studies have been reported on relationships between SAW input parameters and HMZ. It is obtained from these researches that heat input plays a major role in hardness [13, 14].

The combined effect of boehmite nanoparticles surface adsorbed with vanadium (BNV) and welding input parameters on the HMZ has been investigated in the SAW process. Boehmite (γ-AlO(OH)) nanoparticles is a metastable phase of aluminum oxide and its surface is covered with OH groups capable of absorbing materials such as dye, cations, etc. The vanadium solution

UNDER PEER REVIEW

required was obtained from the Bistoon power plant wastewater in Kermanshah province. Further, vanadium cations were extracted from vanadium solution and subsequently were adsorbed on the surface of boehmite nanoparticles and were heated up to form BNV powder. Boehmite while adsorbing a large amount of vanadium cations was able to deliver vanadium nanoparticles to the weld pool. First and foremost, due to its nano grain size and high cost, BNV could not be mixed with SAW flux. Furthermore, because the goal was to introduce BNV directly into the weld pool, BNV was first dispersed in ethanol and then applied as a paste to the surface of mild steel plates of various thicknesses prior to welding. The experimental data was collected using a five-level five-factor rotatable central composite design (RCCD). The input parameters were arc voltage (V), welding current (I), welding speed (S), electrode stick-out (N), and BNV (F), and the response was the HMZ. Experiments were carried out, and HMZ values were measured.

2. EXPERIMENTAL METHODS AND PROCEDURES

2.1 Preparation of Boehmite Nanoparticles Surface Adsorbed with Vanadium

Synthesizing of the boehmite nanoparticles used in this work was conducted based on the techniques that are published previously [15]. In summary, solutions of 20 gr of Al $(NO_3)_3.9H_2O$ in 30 ml distilled water and 6.490 gr of NaOH in 50 ml of distilled water were made. After then, the aluminum solution received a dose of sodium hydroxide at a rate of 2.94 ml/min for 17 minutes with intensive stirring. Following this, the resulting mixture was placed in an ultrasonic bath for mixing up at a temperature of 25 °C for 3 hours. The precipitate was then filtered and rinsed with distilled water before being stored in an oven at 220 °C for 4 hours. To adsorb vanadium on the surface of boehmite nanoparticles, vanadium solution and boehmite powder were mixed up in 200 ml of water for 24 hours according to Fig. 1.

UNDER PEER REVIEW

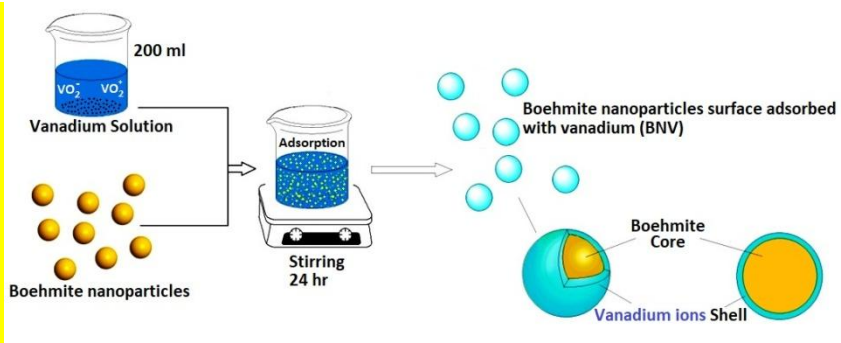

Fig. 1. Adsorption of vanadium on the surface of boehmite nanoparticles

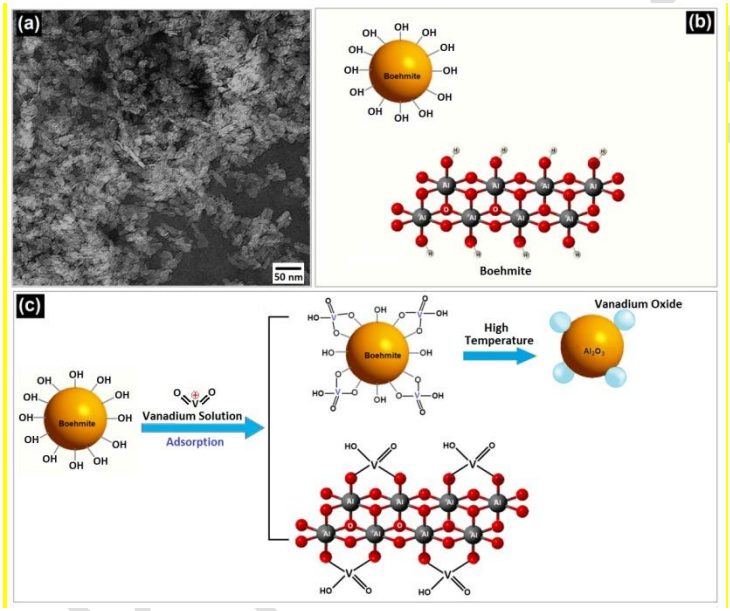

Fig. 2. Structure of boehmite nanoparticles

2.1.1 Boehmite and BNV nanoparticles

Figure 2a shows the TEM image of boehmite nanoparticles having a crystalline structure with 10-30 nm particle size. Figure 2b shows the molecular structure of functionalized boehmite with its surface, being covered with OH groups. These OH groups are capable of adsorbing metal cations. In Fig. 2c, the process of vanadium (VO^{2+}) adsorption by boehmite nanoparticles has been shown.

Figures 3a and 3b show the FTIR spectra of boehmite nanoparticles and BNV, respectively. The stretch frequency of Al-OH is related to the two strong peaks at 3089 cm-1 and 3114 cm-1 in Fig.

3a. Peaks of 735 cm-1, 605 cm-1, and 480 cm-1 are associated with Al-O-Al vibration modes, whereas frequencies of 1070 cm-1 and 1163 cm-1 are associated with symmetrical bonding vibrations of hydrogen bands OH...OH. The stretch vibration of the nitrate (NO3-) impurity in the solution is responsible for the frequency peak of 1384 cm-1. [15].

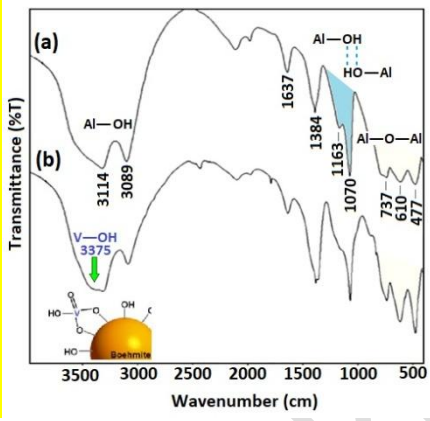

Figure 3. FTIR spectra of synthesized (a) nano-boehmite (b) and BNV

Adsorption of vanadium cations on the surface of nanoparticles did not change the spectrum of boehmite as shown in Figure 3b. It can be seen that the intensity of three peaks (477, 610, 737 cm-1) has increased due to the blocking of some OH groups by vanadium cations and the formation of new oxide bonds. Moreover, the revelation of a new peak at 3375 cm-1 could be linked to V-OH bond stretching vibrations.

2.2 Design of Experiments

Design of experiments is a set of strong techniques for developing new processes, gaining a better understanding of existing processes, and optimizing them to obtain world-class performance. [16]. V, I, N, S, and F were used as input parameters in this study, and experiments were conducted using a five-level five-factor RCCD of experiments. Table 1 shows the results of thirty-two experiments based on the design matrix. The coded values were calculated by equation (1):

$$X_i = 2[2X-(X_{max}+X_{min})]/(X_{max}-X_{min}) \quad (1)$$

UNDER PEER REVIEW

The required coded value of a parameter "X" is Xi. X is any parameter value between Xmin and Xmax, and Xmin and Xmax are the input parameters' minimum and maximum levels, respectively. Table 2 lists the input parameters and their associated coded levels.

Table 1. Design matrix for experiments

No.	V	I	N	S	F	Experimental HMZ	No.	V	I	N	S	F	Experimental HMZ
1	0	0	0	0	0	150.100	17	0	0	0	0	0	151.268
2	0	0	0	-2	0	143.792	18	-1	1	1	-1	1	144.982
3	-1	1	-1	1	1	149.462	19	0	0	0	0	2	161.245
4	-1	-1	1	1	1	168.094	20	1	1	1	1	1	152.565
5	1	1	1	-1	-1	133.103	21	1	-1	-1	-1	-1	142.580
6	0	2	0	0	0	139.354	22	1	-1	1	-1	1	152.740
7	1	1	-1	1	-1	139.748	23	-2	0	0	0	0	166.593
8	0	0	-2	0	0	148.311	24	0	0	0	0	0	150.103
9	-1	-1	-1	-1	1	157.440	25	1	-1	-1	1	1	152.430
10	1	1	-1	-1	1	152.153	26	0	0	0	0	0	150.915
11	-1	-1	1	-1	-1	159.816	27	-1	1	-1	-1	-1	151.247
12	0	0	0	0	0	151.174	28	-1	1	1	1	-1	156.127
13	0	0	0	0	-2	142.738	29	0	0	0	2	0	155.008
14	-1	-1	-1	1	-1	159.441	30	2	0	0	0	0	141.129
15	1	-1	1	1	-1	154.153	31	0	0	2	0	0	153.657
16	0	0	0	0	0	151.621	32	0	-2	0	0	0	164.222

Table 2. The range of input parameters

Parameter	Notation	Units	Coded values				
			-2	-1	0	+1	+2
Arc voltage	V	[Volt]	24	26	28	30	32
Welding current	I	[Amp]	500	550	600	650	700
Electrode stick-out	N	[mm]	30.0	32.5	35.0	37.5	40.0
Welding speed	S	[mm/min]	300	350	400	450	500
Thickness of BNV	F	[mm]	0.00	0.25	0.50	0.75	1.00

Low carbon steel plates were cut into test pieces with dimensions of 150 mm x 50 mm x 15 mm and their sides were cleaned before welding. In addition, work-piece surfaces were coated with layers of BNV powder prior to welding. The experiments were performed on specimens utilizing an automated SAW machine, as illustrated in Fig. 4, which used direct current with reverse polarity and the bead-on-plate approach to place 32 welds. The chemical composition of base metal is presented in Table 3. An abrasive cutter was used to cut each sample transverse to the

UNDER PEER REVIEW

welded joint. Ordinary metallurgical polishing technique was used for preparing the samples and etched with standard 2 % Nital. Hardness examinations were carried out by the ASTM E92 standard in the melted zone of welds. Each sample was given five measurements, with the average value being used as a data point. Figure 5 shows a sample of the melted zone of the weld with hardness points.

Table 3. Base metal chemical composition

Element	Cr	P	S	Si	Ti	Mn	C	Fe
% W	0.031	0.007	0.01	0.024	0.002	0.417	0.113	Balance

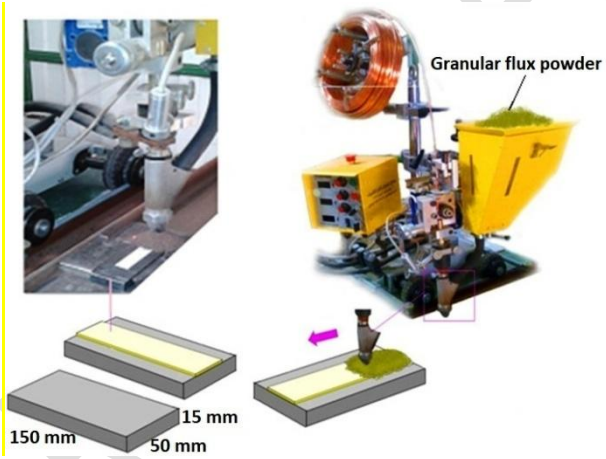

Fig. 4. Experimental setup

Fig. 5. Weld melted zone

UNDER REVIEW

3. RESULT AND DISCUSSION

3.1 Presence of Nanoparticles in the Weld Melted Zone

Firstly, SEM and EDS spectrum methods were used to prove that BNV nanoparticles were

entered into the weld melted zone. Figure 6 shows that boehmite nanoparticles' surface adsorbed with vanadium are agglomerated owing to high temperatures in the weld pool, forming agglomerates of 500 nm to 2 µm in diameters. The EDS spectrum of these agglomerates confirms the presence of a tiny amount of vanadium on the surface of boehmite nanoparticles. Dark elliptical particles seen in the SEM micrograph are inclusions developed in the weld metal due to the presence of SAW flux.

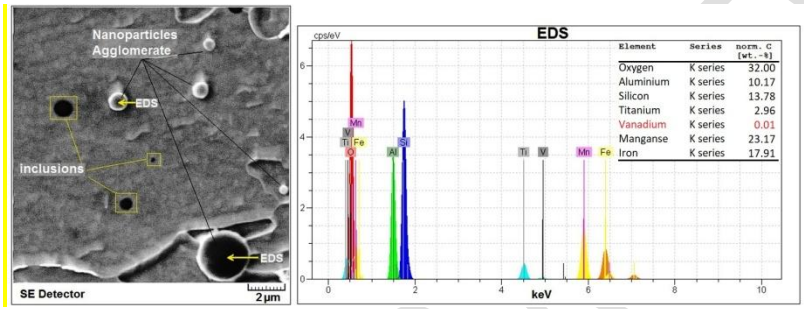

Fig. 6. SEM micrograph of weld metal with its EDS

As shown in Figure 7, for different magnifications, nanoparticles of 100 nm grain size and less would be traced in the weld metal. These nanoparticles due to the escaping agglomeration phenomenon, therefore, were able to be dispersed in the weld metal.

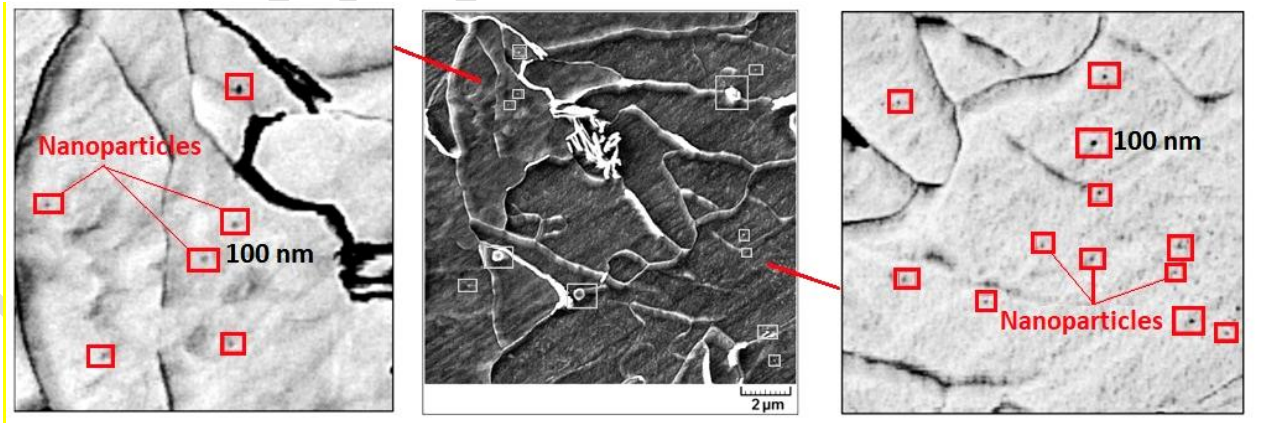

Fig. 7. Vanadium in the weld metal

As it is shown in Figure 8, lightweight elements have a darker contrast as compared with heavier ones. Because the backscatter in heavy elements with higher atomic numbers is stronger than light elements with lower atomic numbers, making them look brighter in the picture.

Backscattered electrons are utilized to identify differences in chemical composition across zones [17]. As can be seen, in areas surrounding some of the dark particles, there is a bright layer showing a core-shell structure having different chemical compositions. EDS spectrum of particle agglomerations shows the presence of a little amount of vanadium element in that structure. The brighter region surrounding agglomeration is due to vanadium oxide.

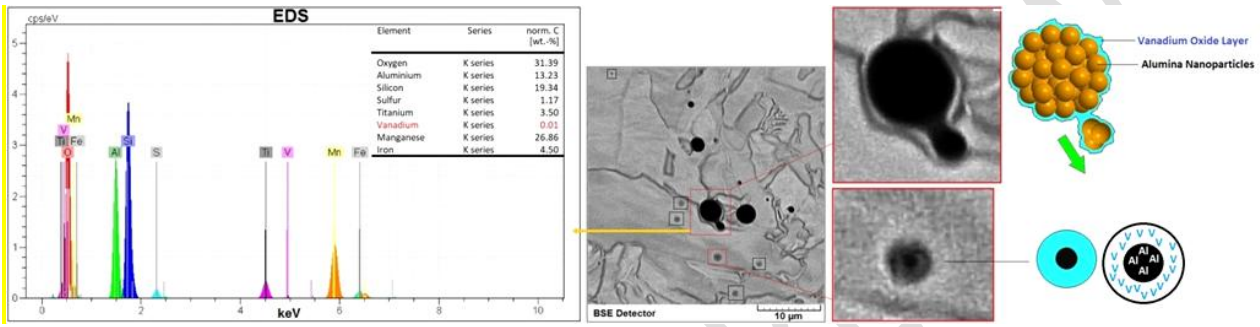

Fig. 8. Core-shell structure of boehmite and vanadium nanoparticles

Figure 9 shows another BSE micrograph which, provides us with more accurate information. As it is observed above, particles identified as A show aluminum oxide nanoparticles and vanadium oxide nanoparticles, which are developed in the form of a core-shell structure owing to the high temperature in the weld pool. Particles identified as B show nanoparticles of vanadium oxide, which is either due to very tiny nanoparticles with boehmite coring or simply separated from the surface of the core-shell structure. Furthermore, particles identified as C indicate inclusions without having any sort of shell.

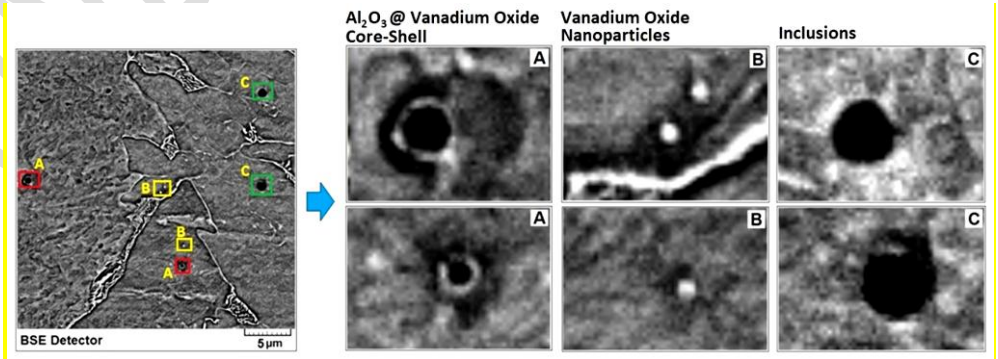

Fig. 9. BSE micrograph of the melted zone

3.2 Main Effects of Input Parameters

Figure 10 shows the main effects of input factors on the HMZ. Figure 10a depicts that when arc voltage increased, the HMZ decreased. The heat input into the weld pool increased when the arc voltage was increased. Heat input has a crucial effect in arc welding processes such as the SAW process since it influences the cooling rate like preheating and inter-pass temperature, affecting the weld metal's microstructure and mechanical properties. Higher heat input leads to a lower cooling rate and an increase in the solidification time which encourages the growth of larger grains, indicating a decrease in the HMZ.

As can be seen in Figure 10b, the HMZ decreased when the welding current has been increased. The microstructure of weld metal is mainly controlled by heat input to the weld pool and the rate of cooling. Increasing the welding current resulted in more heat being delivered into the weld metal. The cooling rate decreased as the heat input increased, and as a result, the time for solidification increased, resulting in coarser grains. Lower hardness is usually indicated by coarser granules in microstructure.

Figure 10c shows that the HMZ increased with an increase in sick-out. Increasing the length of electrode stick-out will lead to increase electrical resistance, which lowered heat input into the weld pool, resulting in a longer solidification period and hence increasing the HMZ.

The HMZ increased with rising welding speed as presented in Figure 10d. This increase might be attributable to the fact that increasing increase in the welding speed reduces the amount of heat input into the workpiece, and subsequently decrease the cooling rate. Higher hardness is due to this fall in the cooling rate which yielded fine grains.

The HMZ increased with an increase in the thickness of BNV, as shown in Figure 10e. When BNV was added to the weld pool, some amount of vanadium nanoparticles was released in this area which resulted in the transformation of polygonal ferrite to acicular ferrite. Figures 11a and 11b show optical micrographs of the microstructure of weld metal. From Figure 11b, it is clear

UNDER PEER REVIEW

that the amount of acicular ferrite increased with the increase in the thickness of BNV. Toughness and hardness are increased as a result of a higher percentage of acicular ferrite and finer grain size, as stated elsewhere [18, 19]. On the other hand, vanadium affects the austenite in the weld puddle by lowering its carbon solubility [18]. This results in an increase in the amount of vanadium carbides in the weld puddle which increases the hardness. Moreover, another mechanism that would explain the increase in the HMZ is probably due to standard strengthening mechanisms, such as grain refinement during solidification or oxide dispersion strengthening (i.e. introducing hard particles into the microstructure). Fine-grained materials are stronger and harder than coarse-grained materials because fine-grained materials have more grain boundaries, which restrict dislocation motion. In fact, according to the Hall-Petch equation, if the grain size decreases, there is greater resistance for a motion of dislocations due to increased grain boundary area and frequent change in orientation of slip planes due to the misorientation of grains. Hence larger stress would be required to move dislocations. This would imply that the strength of the material has increased. Indeed, by refining the grain size and enhancing the oxide dispersion, many of the essential mechanical characteristics of steel, including hardness, may be enhanced, as in our case over here.

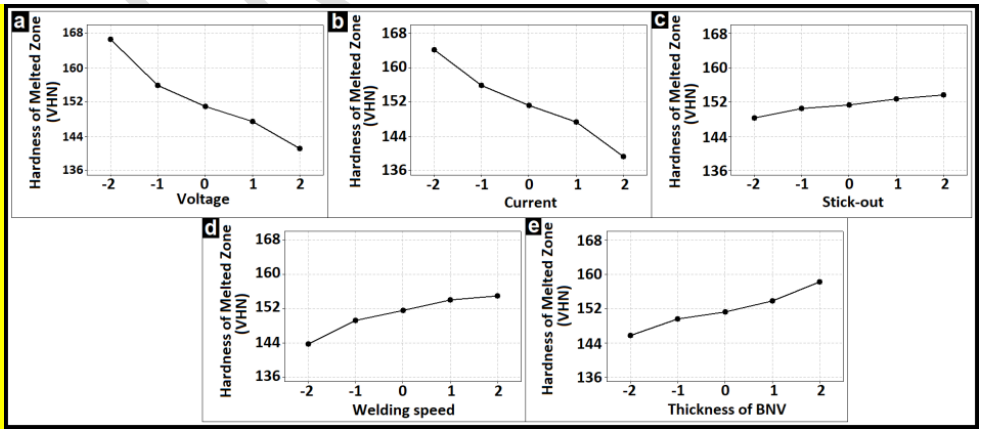

Fig. 10. Main effects of input parameters on HMZ

UNDER PEER REVIEW

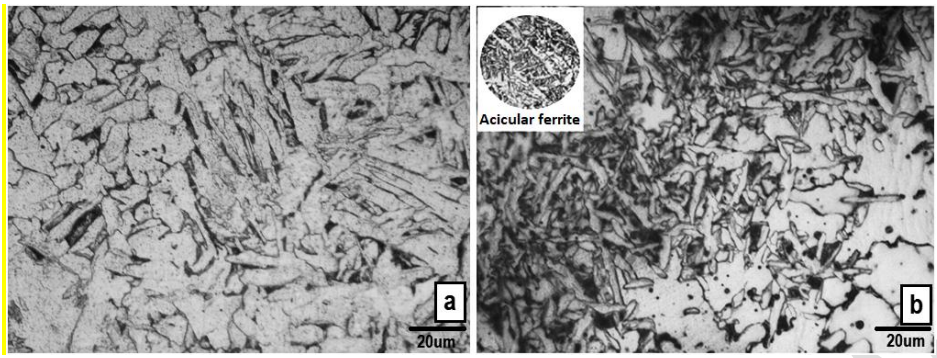

Fig. 11. Optical micrographs of the melted zone microstructure at various thicknesses of BNV (a) 0.0 mm (b) 1.0 mm

Figure 12 shows the SEM micrograph for the surface of the core-shell structures, where a thin layer of vanadium oxide of nano-meter scale covering the alumina core, which is being responsible for the nucleation and formation of acicular ferrite structure giving an optimum toughness and strength combination in weld metal [19].

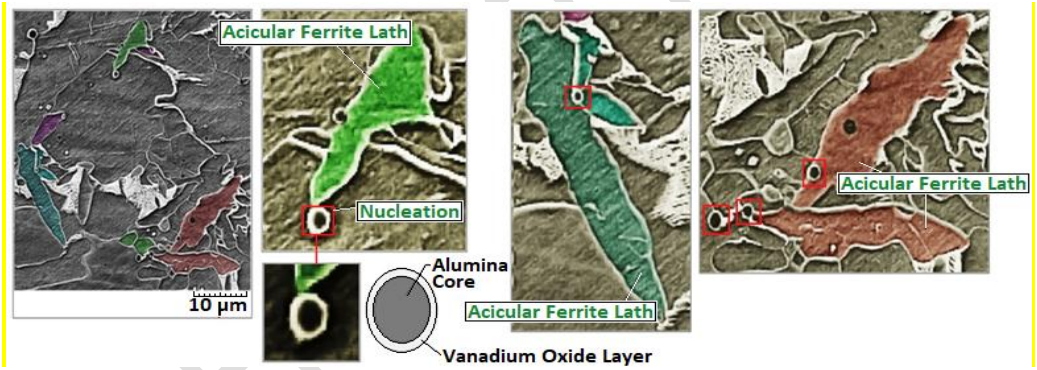

Fig. 12. Formation of acicular ferrite by a shell of the Core/ Shell structure

4. CONCLUSIONS

In this research, an attempt was made to introduce a novel approach for delivering vanadium nanoparticles to the weld pool with the help of cheap boehmite nanoparticles. SEM micrograph and EDS tests from weld puddle of experiments were conducted to validate that nanomaterials were input into the melted zone. In addition, the main effects of welding input parameters and nanomaterials on HMZ were evaluated for the SAW process.

The following is a summary of the study's findings:

UNDER PEER REVIEW

i. Arc voltage and welding current had the major effect which resulted in decreasing hardness of welded zone significantly.

ii. Speed of welding speed and electrode stick-out had less effect on hardness than arc voltage and welding current. The HMZ increased with the increase in welding speed and electrode stick-out.

iii. Increasing the amount of boehmite nanoparticles surface adsorbed with vanadium leads to an increase in HMZ considerably.

iv. The HMZ obtained for the weld samples were found to correspond to the formation of more acicular ferrite in the weld metal due to the addition of BNV to the weld pool.

UNDER PEER REVIEW

REFERENCES

1. Ghosh A, Chattopadhyay H. Mathematical modeling of moving heat source shape for submerged arc welding process. Int J Adv Manuf Technol. 2013;69:2691–2701
2. Wang ZQ, Wang XL, Nan YR, Shang CJ, Wang XM, Liu K, Chen B. Effect of Ni content on the microstructure and mechanical properties of weld metal with both-side submerged arc welding technique. Mater Charact. 2018;138:67–77
3. Singh B, Khan ZA, Siddiquee AN, Maheshwari S. Effect of CaF_2, FeMn and NiO additions on impact strength and hardness in submerged arc welding using developed agglomerated fluxes. J Alloys Compd. 2016;667:158–169. https://doi.org/https://doi.org/10.1016/j.jallcom.2016.01.133
4. Kazemi M, Aghakhani M, E. H-J, Behmaneshfar A. Optimization of the Depth of Penetration by Welding Input Parameters in SAW Process Using Response Surface Methodology. Metall Mater Trans B. 2016;47B:714–719. https://doi.org/10.1007/s11663-015-0492-x
5. Pal TK, Maity UK. Effect of nano size TiO_2 particles on mechanical properties of AWS E 11018M type electrode. Mater Sci Appl. 2011;2:1285–1292
6. Fattahi M, Nabhani N, Vaezi MR, Rahimi E. Improvement of impact toughness of AWS E6010 weld metal by adding TiO_2 nanoparticles to the electrode coating. Mater Sci Eng A. 2011;528:8031–8039
7. Chen B, Han F, Huang Y, Lu K, Liu Y, Li L. Influence of nanoscale marble (Calcium Carbonate $CaCO_3$) on properties of D600 R surfacing electrode. Weld J. 2009;88:99-s-103-s

8. Aghakhani M, Naderian P. Modeling and optimization of dilution in SAW in the presence of Cr_2O_3 nano-particles. Int J Adv Manuf Technol 2015;78:1665–1676

9. Aghakhani M, Ghaderi MR, Jalilian MM, Derakhshan AA. Predicting the combined effect of TiO_2 nano-particles and welding input parameters on the hardness of melted zone in submerged arc welding by fuzzy logic. J Mech Sci Technol. 2013;27:2107–2113. https://doi.org/https://doi.org/10.1007/s12206-013-0523-y

10. Yong G, Han D. Review of applications of vanadium in steels. In: Proceedings of International Seminar on Production and Application of High Strength Seismic Grade Rebar Containing Vanadium, Beijing, China, 2010; 1–11

11. Jiang M, Li ZX, Wang YJ, Shi YW, Jiang JM, Li XB. Effect of vanadium on microstructures and properties of Fe--Cr--C self-shielded metal cored hardfacing alloys. Sci Technol Weld Join. 2008;13:114–117

12. Sage AM. Effect of vanadium, nitrogen, and aluminium on the mechanical properties of reinforcing bar steels. Met Technol. 1976;3:65–70

13. Yang Y. The effect of submerged arc welding parameters on the properties of pressure vessel and wind turbine tower steels. University of Saskatchewan; 2008.

14. Kolhe KP, Datta CK. Prediction of microstructure and mechanical properties of multipass SAW. J Mater Process Technol 2008;197:241–249

15. Rajabi L, Derakhshan AA. Room temperature synthesis of boehmite and crystallization of nanoparticles: effect of concentration and ultrasound. Sci Adv Mater. 2010;2:163–172

16. Antony J. Design of experiments for engineers and scientists. Elsevier; 2014.

17. Goldstein JI, Newbury DE, Michael JR, et al (2017) Scanning electron microscopy and X-ray microanalysis. Springer

18. Baker TN. Processes, microstructure and properties of vanadium microalloyed steels. Mater Sci Technol. 2009;25:1083–1107

19. Babu SS. The mechanism of acicular ferrite in weld deposits. Curr Opin Solid state Mater Sci. 2004;8:267–278

UNDER PEER REVIEW